

# Environmental Testing of the HERMeS TDU-2 Hall Thruster

Robert B. Lobbia,<sup>\*</sup> Ryan W. Conversano,<sup>†</sup> Sean Reilly,<sup>‡</sup> Richard R. Hofer,<sup>§</sup> and Ryan Sorensen<sup>\*\*</sup>

*Jet Propulsion Laboratory, California Institute of Technology, Pasadena, CA 91109*

The Hall Effect Rocket with Magnetic Shielding (HERMeS) is a 12.5 kW magnetically shielded Hall thruster presently under development for deep-space missions. A development model HERMeS thruster, TDU-2, with borosilicate channel walls, has successfully undergone proto-qualification testing including random vibration and thermal-vacuum, demonstrating the thruster can survive critical launch and operational environmental requirements. The three-axis random vibrational tests were performed with the thruster body mounted directly to the shaker table using a modified loading schedule to compensate for the vibration isolation dampers under design for the flight thruster. Initial random vibration testing revealed issues with fragmentation of magnetic coil potting material and thruster spool mount fabrication weaknesses that were addressed with an alternate potting material and fabrication revisions that were then successfully retested with an additional round of random vibration tests. Thermal-vacuum testing involved three cycles of full-power 600 V 12.5 kW thruster operation from  $-121^{\circ}\text{C}$  to  $+373^{\circ}\text{C}$  which included eight hours at peak temperature as well as a hot restart. A thermal model of the test configuration was developed and validated with the experiment results within an average difference of  $5^{\circ}\text{C}$ . Before and after the random vibrational and thermal-vacuum tests, the thruster performance, plasma plume, thrust vector angle, discharge characteristics, and magnetic field profile were measured. The thruster performance, magnetic field, and most other parameters remained invariant throughout the environmental testing campaign. During the thermal testing, an increase in the discharge oscillation amplitude of 11% was observed as well as subtle thrust vector changes of  $\pm 0.2^{\circ}$  as the thruster warmed from  $-121^{\circ}\text{C}$  to  $+373^{\circ}\text{C}$ .

## I. Introduction

ENVIRONMENTAL testing of electric propulsion thrusters is an essential part of qualifying the devices for the flight environment [1]. Hall thrusters have unique structural and thermal challenges as relatively mass-dense devices with low thermal conductivity that operate at steady-state temperatures in excess of  $350^{\circ}\text{C}$  [2].

## II. Test Setup and Approach

### A. TDU-2 HERMeS Thruster

The Technology Development Unit-2 (TDU-2) HERMeS thruster is one of three TDU thruster presently undergoing a series of risk reduction and wear test efforts at NASA GRC and JPL. Each of the thrusters is nearly identical with the exception that the TDU-2 and TDU-3 thrusters now employ borosilicate ceramic channel walls while the TDU-1

---

<sup>\*</sup> Engineer, Electric Propulsion Group, Senior Member AIAA, robert.b.lobbia@jpl.nasa.gov .

<sup>†</sup> Engineer, Electric Propulsion Group, Member AIAA.

<sup>‡</sup> Engineer, Thermal Engineering Group, Member AIAA.

<sup>§</sup> Supervisor, Electric Propulsion Group, Associate Fellow AIAA.

<sup>\*\*</sup> Engineer, Dynamics Environments Group.

retains boron nitride. Each TDU thruster is nominally a 12.5 kW magnetically shielded Hall thruster with a throttle curve that extends down to 3 kW and includes voltages from 300-700 V with a projected lifetime requirement in excess of 23,000 hours. A proto-flight version of this HERMeS thruster, the EDU (Engineering Development Unit), is presently under design and fabrication at Aerojet Rocketdyne for planned integration on the Power and Propulsion Element (PPE) module of the lunar space station or “deep-space gateway” NASA is developing with a present launch date estimated in the  $\approx 2022$  timeframe [3].

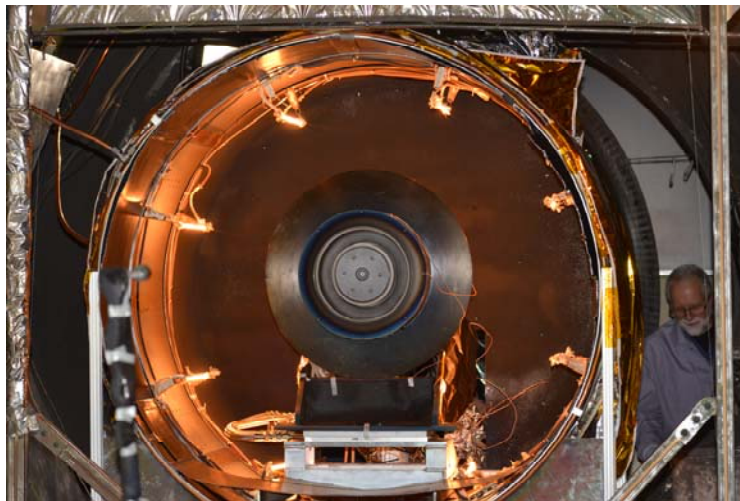
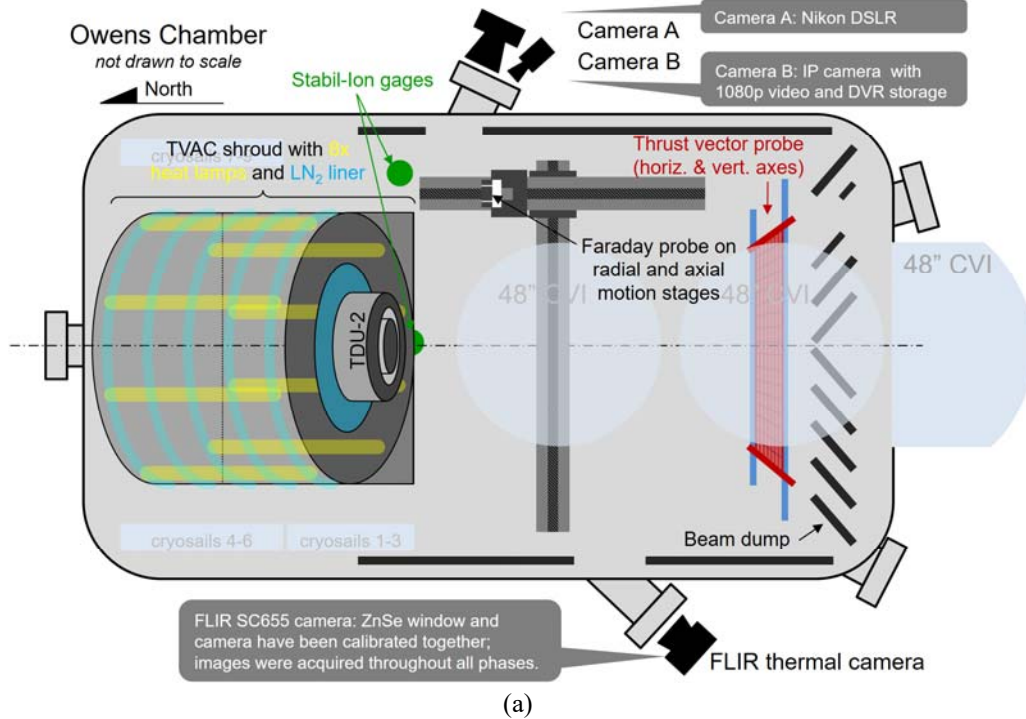


**Figure 1. (a) Schematic of TVAC test setup and (b) TDU-2 thruster installed in TVAC shroud inside Owens test facility performing heat lamp check.**

### B. Owens Vacuum Facility

The JPL Owens test facility is a 3-m diameter 8.6-m long cylindrical vacuum chamber that utilizes 3x 48” CVI cryopumps and 9x custom LN<sub>2</sub> shrouded “cryosail” [4] plates. The facility pumping speed varied slightly from

230,000 to 260,000 liters-Xe/s (coldflow measured) for different portions of the included testing with a typical zero-flow base pressure  $<5 \times 10^{-7}$  torr-Xe. Corrected xenon pressures were collected in accordance with the current EP standard [5] using Stabil-Ion gauges and during 600 V 12.5 kW thruster operation, the pressure was typically  $1.2 \times 10^{-5}$  torr-Xe. The chamber walls downstream of the thruster are lined with graphite panels and a baffled set of graphite beam dump panels reduce the backsputter rate (predominantly carbon in the axial direction near the TDU-2 thruster), for 600-V 12.5-kW operation, to 4.1 nm/hr ( $\pm 0.5$  nm/hr, see Ref. [6]) as measured by a temperature controlled QCM (Quartz Crystal Microbalance).

The TVAC Test 2 performed in early 2018 for this effort was the first test conducted after a significant upgrade of the Owens test facility that involved: installing 9 new cryogenic pumps, installation of a new water chiller (and plumbing), the addition of 5 new vacuum flanges, new LN<sub>2</sub> vacuum jacketed plumbing, new LN<sub>2</sub> keepfulls, addition of new building electrical power, and other improvements. After these upgrades, various cryogenic stability issues occurred in addition to problems with some of the new facility components that delayed the TVAC testing by several months. The unique TVAC setup with the large (>1 m diameter) shroud inside the 3 m diameter Owens facility place this surface in unusually close proximity to six of the facility cryosail pumps and several initial attempts to reach full power thermal equilibrium resulted in overheated cryo surfaces that necessitated stopping the test to modify the setup and replace these cryosails with smaller—more thermally stable—units. The Owens facility had few issues TVAC testing the 7-kW NEXT ion engine up to it maximum qualification temperature of +215°C [1]. At nearly double the discharge power and an additional +158°C (or +373°C maximum) qualification test temperature, the HERMeS thruster TVAC testing proved more challenging but still perfectly feasible.

### C. Thruster Testing Instrumentation

Throughout all phases of thruster operation in the JPL Owens test facility, standard low-speed and high-speed thruster telemetry are recorded and monitored. The low-speed telemetry includes all the calibrated sense lines on the DC power supplies (main discharge, inner magnet, outer magnet, cathode heater and cathode keeper), cathode to ground bias, body current, facility pressure, cryogenic vacuum pump temperatures, water coolant temperatures, propellant flow rates (anode and cathode), thrust vector probe currents, and more (160 channels in all).

The TVAC portion of this this test campaign includes a total of 22x type-K thermocouples (TCs) mounted to the following locations on the TDU-2 thruster and TVAC shroud: (1) control TC (on backpole near cathode bore; see Figure 15(b)), (2) inner core, (3) inner screen, (4) outer screen, (5) backpole near ID (control TC backup), (6) outer front pole, (7) front pole cover, (8) outer guide, (9) radiator inside spool, (10) radiator mid-fin, (11) radiator OD #1, (12) radiator OD #2, (13) back cover mid, (14) spool mount mid, (15) propellant line, (16) TVAC shroud 2:00, (17) TVAC shroud 6:00, (18) mount base, (19) MLI garage door motor, (20) power harness tip, (21) power harness mid, and (22) TVAC shroud outer MLI. These TCs have a nominal accuracy of  $\pm 2.2^\circ\text{C}$  or  $\pm 0.75\%$  (whichever is larger) but they are all recorded by an OPTO22 based data-logger with an accuracy of  $\pm 3^\circ\text{C}$  with the exception of the control TC that is logged by a Keysight 34970A with  $\pm 1.5^\circ\text{C}$  accuracy.

The high-speed thruster telemetry is all routed to an eight channel 12-bit Teledyne LeCroy HDO8000 series oscilloscope and includes the anode current ( $I_a$ ), cathode current ( $I_c$ ), body current ( $I_b$ ), anode to cathode bias ( $V_{a2c}$ ), cathode to ground bias ( $V_{c2g}$ ), and keeper to cathode bias ( $V_{k2c}$ ). High-speed ( $\geq 20$  MHz bandwidth) current measurements are performed using Pearson Electronics model 410 current transformers while high-speed ( $\geq 70$  MHz bandwidth) voltage measurements are performed with active high-voltage differential probes (PICO TA043 or TA044). The signal statistics (peak-to-peak, mean, standard deviation, etc.) are continuously logged while full scope traces (0.1 – 0.5 second windows at 100 MHz) are collected every hour or every thruster condition change.

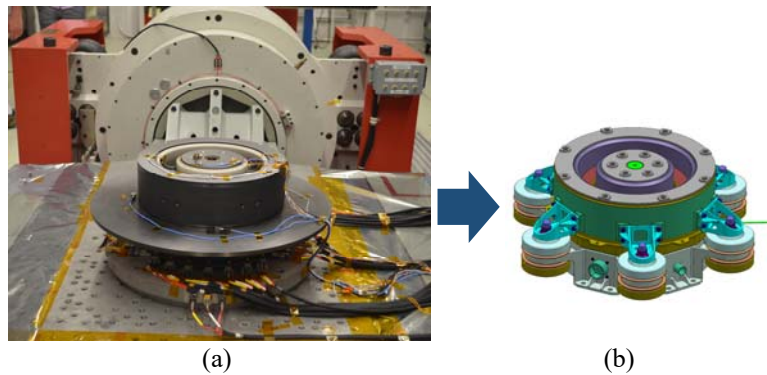


**Figure 2. (a) Accelerometer instrumented TDU-2 mounted on X-Y random-vibration shake table at the JPL Environmental Test Laboratory in 2017. (b) EDU thruster model includes 6 shock isolators and the RV load inputs were modified to account for these.**

#### D. Multi-axis Random Vibration Setup

Two separate configurations of the TDU-2 thruster underwent random vibration (RV) testing during different efforts in 2016 (failed test) and 2017 (successful test). Only setup details specific to the later, 2017 RV testing, are included next. A total of 14 accelerometers were affixed to the thruster (sensors are glued to Kapton™ patches applied to thruster surfaces) as shown in Figure 2(a). Two control accelerometers and one monitor accelerometer are used to control input to shaker table. The evolution of the HERMeS thruster design from the TDU-2 to the EDU led to the inclusion of 6 shock isolators as shown in Figure 2(b). To account for the reduced loading the thruster components—particularly the ceramic channel walls—the load schedule was modified using a FEM thruster model. This enables the TDU-2 thruster components to undergo RV qualification level testing (see Table 1 and Figure 3) that is representative of the levels the EDU thruster components would endure. This imperfect test will still provide valuable insight into potential thruster design weaknesses especially the new addition of the borosilicate ceramic and the consideration that the TDU-2 is the largest (and most massive) Hall thruster to undergo RV testing to date [7].

**Table 1. Qualification level random vibration spectrum schedule.**

Frequency (Hz)	Signature Level (g <sup>2</sup> /Hz)	Qual. Level (g <sup>2</sup> /Hz)	Response Limit (g <sup>2</sup> /Hz)
20	0.001	0.052	3
50	-	0.13	-
150	-	-	3
450	-	-	0.04
500	-	-	0.04
600	-	0.13	-
2000	0.001	0.012	0.012
Overall	0.445 g <sub>rms</sub>	11.4 g <sub>rms</sub>	
Duration	60 seconds	120 seconds	

RV testing is conducted one axis at a time and in the following sequence (for each axis): (1) signature run → (2) -18 db run → (3) -12 dB run → (4) -6 dB run → (5) 0 dB full input run → (6) signature run. Between each run the data and thruster are evaluated prior to proceeding the next run to ensure structural changes are not occurring.

#### E. Environmental Test Sequence

The overall TDU-2 environmental test campaign sequence is presented in Figure 4. The presented process does not include earlier environmental testing when the TDU-2 design included boron nitride (BN) channel walls. Lessons learned from those portions shall be presented later on in this report. After the installation of the new borosilicate channel walls and new magnetic coil assemblies, the thruster was inspected, its magnetic field mapped, and basic performance testing conducted. The RV testing and the TVAC testing are buffered by these same measurements to enable capturing any thruster changes throughout the environmental test effort.

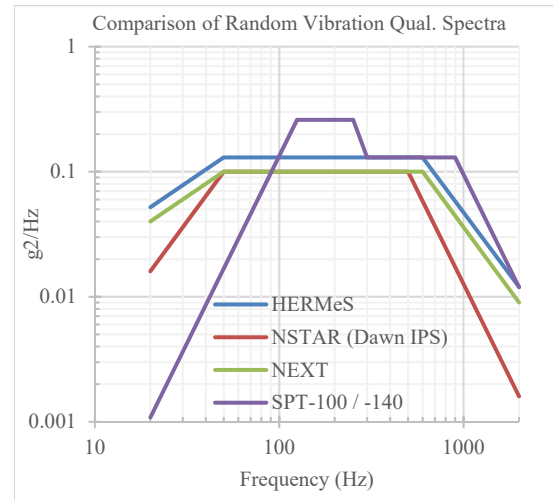


**Figure 3. Random vibration schedule for HERMeS compared to other qualified flight EP systems [1] [7].**

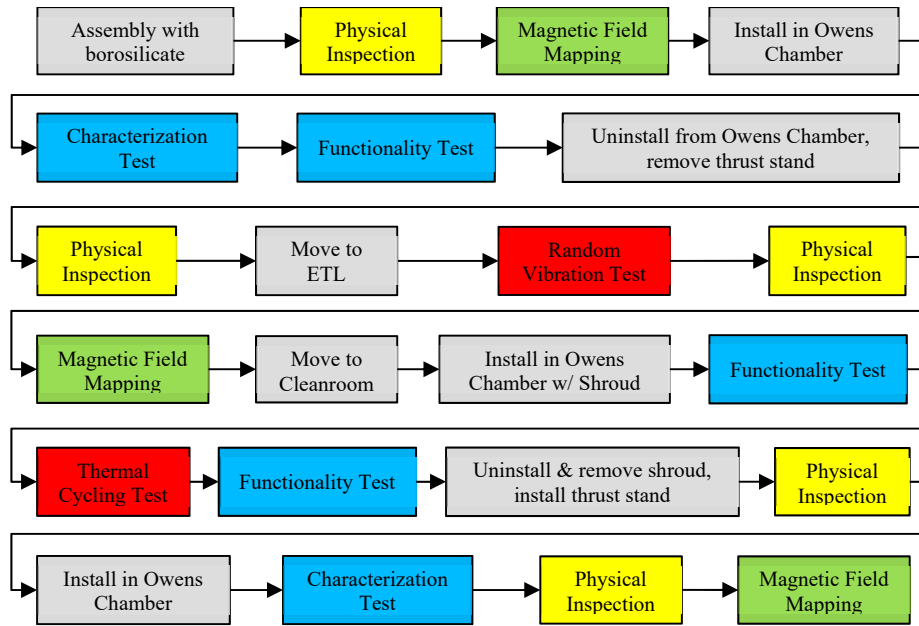


Figure 4. Block diagram overview of TDU-2 environmental testing campaign.

### 1. Functional and Characterization Testing

To assess the thruster characteristics in a consistent manner—to facilitate comparisons between different portions of the environmental test campaign—two sets of tests were devised: “Characterization” and “Functional.” The key measurements for each of these tests are summarize in Table 2:

Table 2. Measurement breakdown for Characterization and Function tests with TDU-2

	Functional	Characterization
Purpose	Check for changes in thruster behavior between environmental tests	Full characterization of thruster performance and behavior
Test Points (AEPS throttle curve)	<b>4 points</b> (from AEPS throttle curve: 300, 400, 500 and 600 V at 20.8 A)	<b>7 points</b> (4 points from AEPS throttle curve and 700V/12.5kW, 500V/12.5kW, 300V/3.1kW)
Thermal Condition*	2 h operation before data collection for thermal baseline	2 h operation before data collection for thermal baseline
Low-speed telemetry	All standard DC signals	All standard DC signals
High-speed telemetry	6 scope channels: $V_{a2c}$ , $V_{c2g}$ , $V_{k2c}$ , $I_a$ , $I_c$ , and $I_b$ (mean, Pk-Pk, standard deviation, scope traces), 20-70 MHz bandwidth	6 scope channels: $V_{a2c}$ , $V_{c2g}$ , $V_{k2c}$ , $I_a$ , $I_c$ , and $I_b$ (mean, Pk-Pk, standard deviation, scope traces), 20-70 MHz bandwidth
Thrust Stand	<b>No</b>	<b>Yes</b>
Far-Field Faraday Probe	Yes	Yes
Thrust Vector Probe	Yes	Yes

\*Thruster bake-out completed before any performance testing

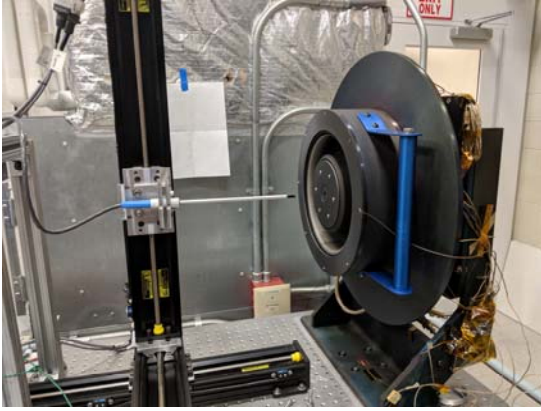


**Figure 5. Automated 3-axis magnetic field mapper setup used to verify pre- and post-vibe/TVAC fields.**

## 2. Magnetic Mapping

A Lakeshore 460 3-axis Gaussmeter probe attached to an automated 3-axis motion stage setup performs thruster magnetic field mapping measurements (Figure 5). Probe to thruster alignment is performed with an accuracy  $\pm 0.25$  mm and grid resolution is set to 1 mm for 2D maps and 0.1 mm for 1D scans. The calibrated Gaussmeter accuracy is  $\pm 0.10\%$  of each measurement axis. Prior to performing measurements, the TDU-2 magnets are degaussed using reversed coil currents followed by verification of negligible ( $< 1$  Gauss) residual zero-current field. Typical 2D maps of a single plane including one radial half of the thruster and extending from near the anode to approximately one channel width downstream take 4-8 hours to complete with various settling time delays and measurement averaging ( $N_{ave,typ.}=10$ ) performed.

## 3. Thruster Inspections

At various times throughout the environmental test campaign (see Figure 4), the thruster is subjected to a thorough physical inspection. This inspection includes photographic documentation of all exterior (and occasionally interior) components as well as gap measurements at 24 locations to check for component displacements. The use of the new borosilicate ceramic in the TDU-2 motivated the inclusion of a materials science expert examine the thruster at all key intervals as well. The role of these inspections is to capture and document any visual or mechanical changes that may (but are not necessarily expected to) occur to the thruster body, pole face covers, radiator, spool mount, thruster mount, or other components during the environmental test campaign.

## 4. Thermal Vacuum Cycles

The thruster shall be subjected to thermal vacuum testing in general accordance with standard JPL flight qualification thermal testing requirements [8] with allowances for the unique nature of the equipment under test. For instance, this is not considered a formal environmental qualification test since the stacked worst case hot environment to be tested ( $352^{\circ}\text{C} + 21^{\circ}\text{C}$  margin) is not possible to recreate in-test with the device alone. There are also acknowledged cases where the standard requirements are not applicable to Hall thruster tests (e.g. sustained operation at cold temperature limits).

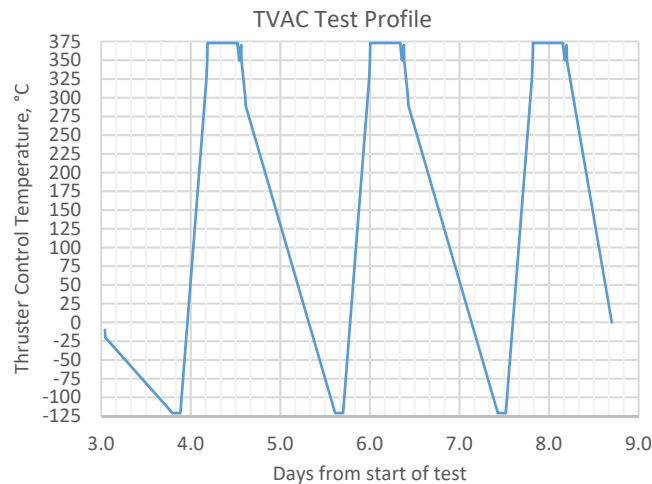


**Figure 6. Thermal cycling profile for TDU-2 TVAC testing.**

The objective of the HERMeS TDU-2 TVAC cycling is to repeatedly expose the thruster to maximal qualification plus margin hot and cold temperatures and demonstrate nominal thruster operation for all environmental states. Temperature data collected during the test shall be used to validate the thermal model of the thruster that may then be

used to predict the temperature response of the thruster in different flight environments. This TVAC effort will test the thruster thermal limits and is also a thermal development test to determine the temperature response of thruster components under different thermal environments and firing conditions.

The test sequence involves chilling the thruster to  $-121^{\circ}\text{C}$  ( $100^{\circ}\text{C} - 21^{\circ}\text{C}$  margin) for an ultra-cold thruster start at full power (600-V 12.5-kW) operation that continues until near-steady state temperatures ( $\approx 350^{\circ}\text{C}$ ) are reached. Then the heat lamps are powered up to increase the thruster temperature to  $+373^{\circ}\text{C}$ . After steady operation—“hot-dwell”—at this temperature for eight hours, the thruster is shut-down and rapidly restarted. The thruster is then shutdown and re-chilled to  $-121^{\circ}\text{C}$  and this cycle repeats twice more. Figure 6 presents the full 3-cycle temperature profile the thruster is subjected to. The thermal model was used to estimate the cooldown and warmup times, but notionally just over 2 days/cycle is expected. The TVAC shroud, shown in Figure 1, includes 8x tungsten quartz infrared heat lamps (nominally rated to 2.2 kW/lamp) whose input power are regulated by a PID temperature controller to a programmed set-point. During the cooldown and cold-soak steps, the lamps are set to operate in survival mode with the thruster temperature controller setpoint at  $-121^{\circ}\text{C}$  while  $\text{LN}_2$  is used to maintain the shroud wall temperature of approximately  $-190^{\circ}\text{C}$ . A MLI (multi-layer insulation) garage door is also lowered during these phases to prevent the warm background chamber surfaces from allowing the thruster to cool down to  $-121^{\circ}\text{C}$ . Predicted and observed cooldown time from near room temperature to  $-121^{\circ}\text{C}$  is roughly 24 hours. After the completion of the cold soak  $\geq 2$  hours at  $-121^{\circ}\text{C}$ , the garage door is opened and the thruster is lit and rapidly brought to full power within 30-60 seconds using standard laboratory power supplies. A low-power heater is used continuously on the garage door motor to enable operation at low temperatures. Another low-power propellant line heater is briefly used just prior to thruster cold-start ignition to prevent the xenon propellant from freezing prior to reaching the thruster propellant manifold. At least 2 hours into the hot-dwell at  $+373^{\circ}\text{C}$ , a limited thruster functional test (limited to only the 600-V 12.5-kW condition) is performed that includes Faraday probe scans at three different axial locations.

### III. Environmental Testing Results

#### F. Random Vibration Test 1 (2016)

An early version of the TDU-2 (boron nitride channel walls) entered RV testing in 2016 and initially failed due to significant particulate emission (reminiscent of NEXT environmental testing [1]), structural changes (warping), large peak mode shifts ( $>30$  Hz and  $>6$  dB), and excessive 8.1% peak damping. After this initial RV test, physical inspections of the thruster revealed multiple out-of-tolerance gaps and magnetic field mapping showed an approximate 8% loss in peak field strength for the same pre-RV coil currents. Thruster disassembly uncovered substantial deterioration of the coil potting material and exposed coil wiring copper on the inner coil as well as several bent stud connectors. Further investigation identified the root cause as drawing and fabrication errors that led to the use of 3 fasteners that were too long (“bottomed out”) to properly secure the inner coil assemble. This left approximately 27 mils of freedom-of-motion for the inner coil bobbin inside the thruster that effectively rattled about during this initial RV test. A variety of thruster design changes were then implemented including use of more robust potting compound, use of non-copper (stainless steel) bobbins, corrected fasteners, improved bobbin studs, and borosilicate channel walls. After rewinding a new set of inner and outer magnet coil bobbins and reassembling the thruster, the environmental testing restarted (e.g. step 1 in Figure 4).

#### G. Random Vibration Test 2 (2017)

In 2017, the updated TDU-2 thruster was excited again in all three axes. This TDU-2 is a slightly modified version that did not successfully pass random vibration in 2016 (Random Vibration Test 1). Since that previous test, it has been decided that the flight design (and EDU) will incorporate shock isolators between the spool mount and the thruster stack up; however these design changes were not present in the TDU-2 model tested in 2016. In order to account for the addition of shock isolators on the EDU HERMeS thrusters, response limiting was used during random vibration testing to simulate expected vibration levels at the isolator-to-thruster interface to avoid over-testing the thruster stack up and discharge channel. In addition, shock testing has been deferred to the EDU thruster units.

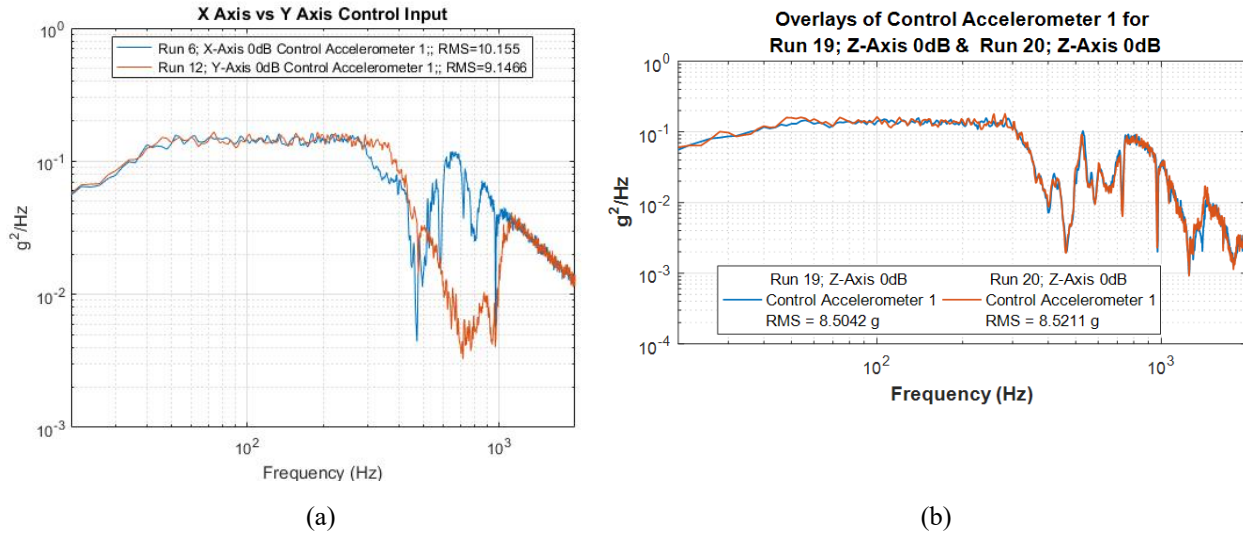
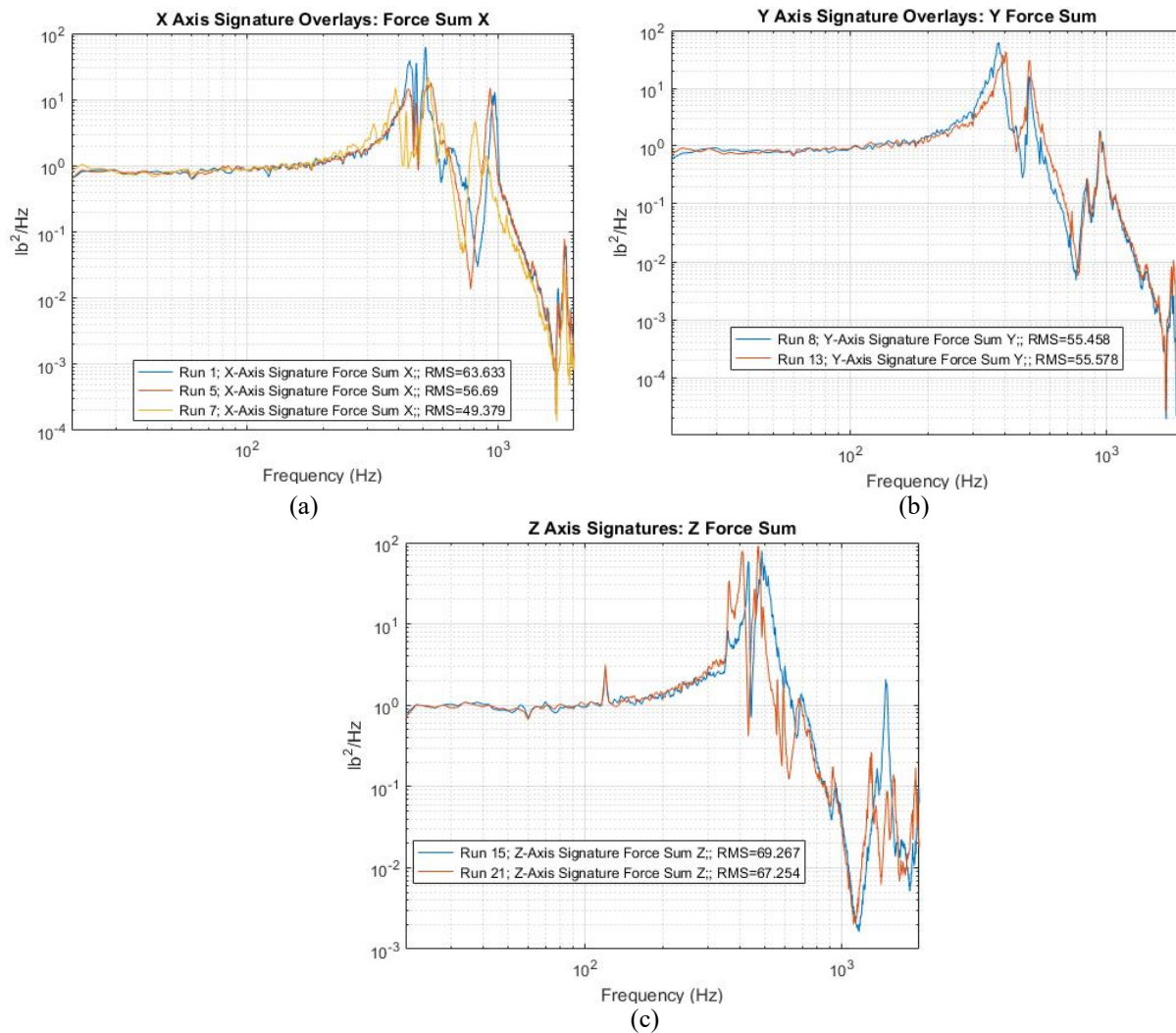


Figure 7. Full RV load input measurements from control accelerometers for (a) X, Y, and (b) Z axes.

During full level testing (Figure 7), the depth of the input notches decreased indicating that the thruster structural response was changing over the duration of the test. This caused an increase in damping and a shift in frequencies, as was expected. No particulate was emitted from the thruster during full level testing of the X and Y axes as it was during the 2016 vibration tests. Minor particulate emission was observed during the Z axis full level testing. The overlays show that the small spectral shifts did continue and damping was slightly higher for the 0 dB run than compared to low level runs. After completing each full two minute run a visual inspection of the thruster was performed and no cracks or other defects were noted in the ceramic discharge channel. While the predicted overall  $g_{rms}$  may compare well with the measured overall  $g_{rms}$ , the shapes differed from FEM (finite element model) predictions because of the structural shifts that occurred during testing. Due to the difference between spectral shapes of the FEM predictions and the full level test the response, loading and response predictions of the ceramic channel are not perfectly relevant since the two structures are not the same. Since the predictions are not ideal representations of the test article, the main metrics to judge the success of the test were the input levels and whether or not the borosilicate channel survived. As evidenced in the pre- vs post-full-level signature runs in Figure 8, minor structural shifts occurred in all three axes, likely caused by a degradation of the potting compound and subsequent stretching and loosening of the magnet coil windings in the inner and outer magnet coils. The potting compound breaking down may have enabled the individual coil turns in the inner and outer coils to move independently which appears to have caused off axis coupling in the lateral excitations and increased overall structural damping.

The thruster design in test will undergo significant changes for the EDU units, thus the main objective of this test was to show that the new borosilicate discharge channel ceramic material can survive exposure to random vibration loading to the levels expected on the EDU units. This key objective of the test was successfully achieved, but during testing some of the same problems from the 2016 RV Test 1 were experienced again. These problems included structural changes for all three axes, shown by imperfectly matching pre- and post-spectral overlays (Figure 8), an increase in overall structural damping as input levels were increased, and minor particulate emission from the inner and outer coils on the Z-axis full-level test. Despite the structural changes observed during testing, the main objective of the test was successfully completed: the thruster stack up was excited to the levels predicted for the EDU thruster units (complete with shock isolators) and the ceramic channel survived with no visible or measured defects.



**Figure 8. Pre- and post-full-level RV signature spectra force sums from all accelerometers for (a) X, (b) Y, (c) Z axes, showing minor structural degradation experienced during the RV testing.**

Immediately following the 2017 RV Test 2, the thruster was inspected and magnetic field mapped with all post-RV measurements matching the pre-RV measurements within uncertainties. The thruster then entered the TVAC portion of the test campaign.

### H. TVAC Test 1 (2017)

The initial attempt to complete TVAC testing with the TDU-2 was halted before the completion of the 1<sup>st</sup> thermal cycle due to failure of an inadequately designed power GSE (ground support equipment) harness. The GSE harness was used to connect the main Owens harness (located outside the TVAC shroud) to the TDU-2 thruster power pigtail. The wiring used for the GSE harness used appropriate gauges for all lines but was constructed of “high-temperature” PVC-nylon-glass insulated cable typically used in aircraft (MIL-W-5086/2-10-9). Unfortunately, the maximum “high-temperature” specification for this PVC cable was only +105°C, and during the infrared lamp heating the insulation melted and sorted the anode line to the grounded TVAC mounting structure. A new high-temperature GSE harness was then constructed of mica and fiberglass insulated furnace wire (type MG) with a maximum service temperature of +450°C. A mock GSE harness section was fabricated with all required cables surrounded by additional fiberglass sleeves all inside a grounded stainless steel conduit and placed in a custom vacuum furnace. This demo high-temperature harness was successfully high-potential tested at 1 kV from 1-10 μtorr and 0-450°C. A full scale version was then built and tested for use as the GSE harness in the TDU-2 TVAC cycles. While the GSE harness issue was remedied, there still remained additional cables inside the thruster that were Kapton™/polyimide insulated

with a maximum rated service temperature of +240°C. Since these cables have been successfully used in thousands of hours of combined TDU-1 -2 and -3 operation at the maximum thruster equilibrium temperature ( $\approx 350^\circ\text{C}$ ), the additional +21°C planned for TVAC qualification was not deemed as an issue (pure polyimides are typically vacuum stable up to  $\approx 400^\circ\text{C}$ ). To mitigate the lamps from adding localized heating to these polyimide insulated cables and the new GSE harness, thin stainless steel foil (with high emissivity and low absorptivity) was added to shadow shield the lamps from these cables and the harness. The GSE harness was also instrumented with two TCs to monitor the cabling temperature.

## I. TVAC Test 2 (2018)

The TVAC test was then resumed, and after sorting out a few facility issues (see section B), a full set of 3 TVAC cycles, as described in section 4, were successfully completed. Necessary water chiller and helium leak repairs occurred between the 1<sup>st</sup> and 2<sup>nd</sup> cycles hence the large temporal gap. The measured thruster temperature profile for these cycles is shown in Figure 9:

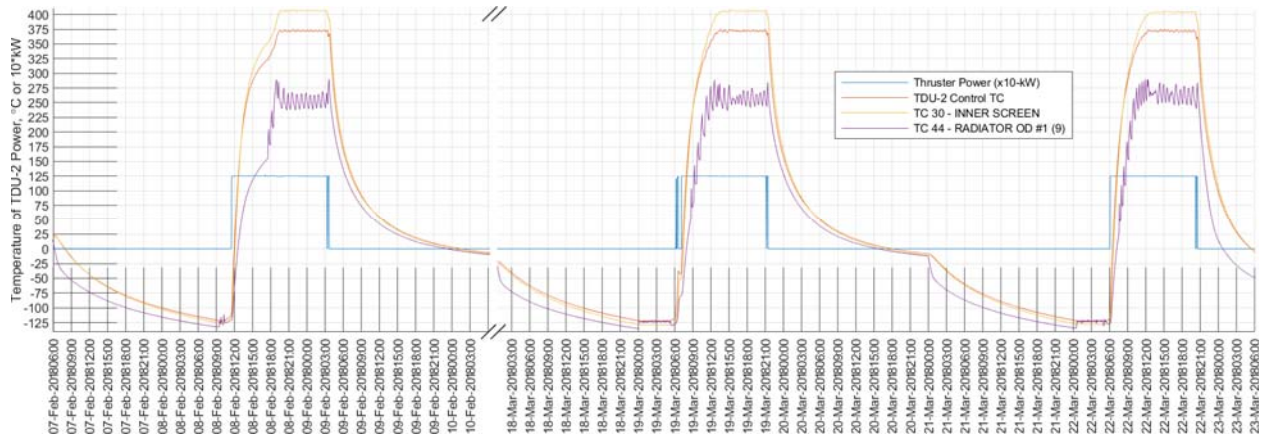


**Figure 9. TVAC testing thermal profile for all 3 cycles with three TCs (Control TC on backpole near cathode bore, inner screen, and outer radiator) and thruster power.**

The Control TC (on the backpole near the cathode bore) was the controlled temperature and the lamp power thermal controller maintained the setpoint temperatures to within  $\pm 1^\circ\text{C}$  at  $-121^\circ\text{C}$  and within  $\pm 3^\circ\text{C}$  at  $+373^\circ\text{C}$ . The other two TC temperatures plotted in Figure 9 are the inner screen and outer radiator. The inner screen was the hottest thruster component that was instrumented for this test while the outer radiator was one of the coolest. The proximity of the outer radiator and large view factor to the heat lamps cause the radiator to react more strongly when the lamps are active as can be seen in the sawtooth like features just before and during the hot-dwell at  $+373^\circ\text{C}$  (as well as when in survival mode near  $-121^\circ\text{C}$ ). Improved controller tuning would limit the “on” or “off” lamp heating “sawtooth” behavior that occurred due to the large ( $\approx 5$  minute) time-response or phase-lag between the “input” lamp power and “output” Control TC. The  $-121^\circ\text{C}$  post-cold-soak startups to full power 600-V12.5-kW operation occurred uneventfully, for all 3 cycles. However, during the first few minutes of full power operation for the 2<sup>nd</sup> cycle, two unexpected thruster shutdowns occurred. The recorded thruster monitor video was reviewed for these shutdowns, close-up thruster photos examined, and all thruster cabling isolations were high-potential tested, but all findings were nominal and the thruster was relit and the cycle resumed without further incident. No other unexpected shutdowns occurred in the TDU-2 TVAC testing. At the conclusion of each 8-hour hot-dwell, the thruster was manually shutdown and relit without issue while the thruster Control TC remained near  $+373^\circ\text{C}$ . The hot-restarts for the first two cycles were performed within 1 minute of shutdown, and the cathode heater was not applied when starting the cathode—only the keeper was used since the cathode was still sufficiently hot to emit electrons. The cathode installed on the TDU-2 for these tested was a  $\text{LaB}_6$  HERMeS hollow cathode while the EDU thruster in development is being designed to use a  $\text{BaO}$  hollow cathode. Since the EDU type cathodes were not available at the time of the TDU-2 TVAC testing, the  $\text{LaB}_6$  cathode was used. It was noted that for the 1<sup>st</sup> and 2<sup>nd</sup> cycle hot-restarts the cathode lighting emitted a few sparks or tiny flares which are not uncommon. For the 3<sup>rd</sup> cycle hot-restart, the cathode was heated for 2.4 minutes prior to lighting and no sparks were observed. This suggests that while the  $\text{LaB}_6$  hollow cathodes can indeed light without additional heating when the thruster is hot, it is recommended to apply some cathode heating to ensure a more benign ignition and limit possible degradation of the  $\text{LaB}_6$  insert.

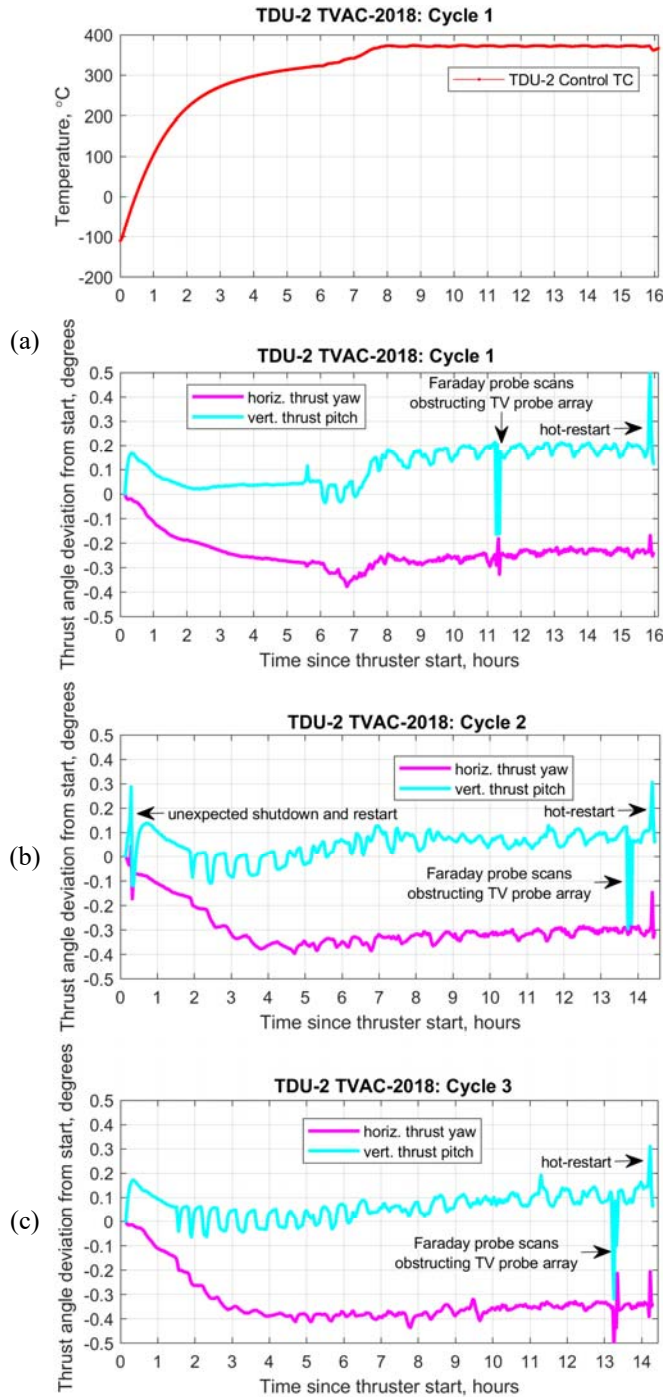


**Figure 10. Thrust vector angle variations throughout TVAC (a) cycle 1, (b) cycle 2, and (c) cycle 3. Control TC temperature from cycle 1 is shown in upper portion of (a) and is notionally similar for cycles 2 and 3.**

$\pm 0.2^\circ$  variation in the horizontal and vertical TV angles respectively for over 14 hours of thruster operation during each cycle while the thruster temperature increased from  $-121^\circ\text{C}$  to  $+373^\circ\text{C}$ . Only the thruster Control TC temperature from the 1<sup>st</sup> TVAC cycle is included in the upper portion of Figure 10(a) since this thermal profile is similar for the following cycles. Event details have been added to Figure 10 to denote when the TV measurements are invalid due to thruster power cycling and Faraday probe scanning which both result in temporarily uneven TV probe rod currents

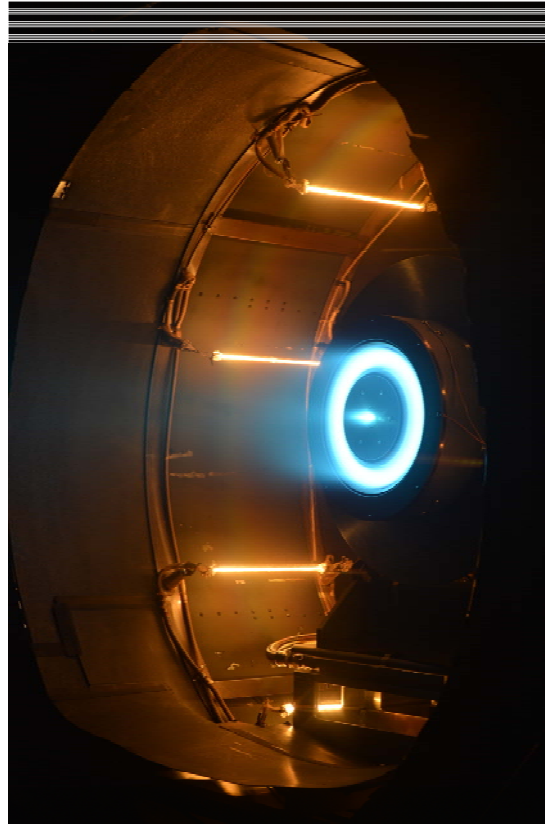


**Figure 11. TDU-2 firing at 600-V 12.5-kW with the thermal heat lamps active and the thruster Control TC at  $+373^\circ\text{C}$ .**

Throughout each of the TVAC cycles an array of 32 cylindrical rods that comprise the JPL thrust vector (TV) probe [9] monitor the instantaneous thrust vector in the horizontal and vertical axes using the centroid of the ion flux. The calibrated thrust vector angular accuracy is approximately  $\pm 0.03^\circ$  and full details on this diagnostic are planned for a future publication. While the absolute angle for the thruster centerline was measured using a calibrated laser alignment jig temporarily bolted to the front of the TDU-2 inner pole, the data presented here are taken relative to the starting TV angle of each cycle thruster firing (e.g.  $0^\circ$  at time = 0 hours since each thruster start). This simplifies the analysis in allowing for direct cycle-to-cycle comparison and ignores minor TV angle thruster component stack-up offsets. The measured TV angle variations for all three TVAC cycles are included in Figure 10. The overall TV profiles are remarkably similar for all three cycles and exhibit approximately  $\pm 0.1^\circ$  and

due to discrete acquisition latencies and physical ion beam obstruction. These small thrust vector angle variations compare well to the STP-140 (Hall thruster) requirement of  $< \pm 0.75^\circ$  [7] and are significantly more stable than the NSTAR [9] and T6 [10] ion thrusters which both exhibit excursions just over  $1^\circ$  while throttling up to full power and approaching thermal equilibrium.

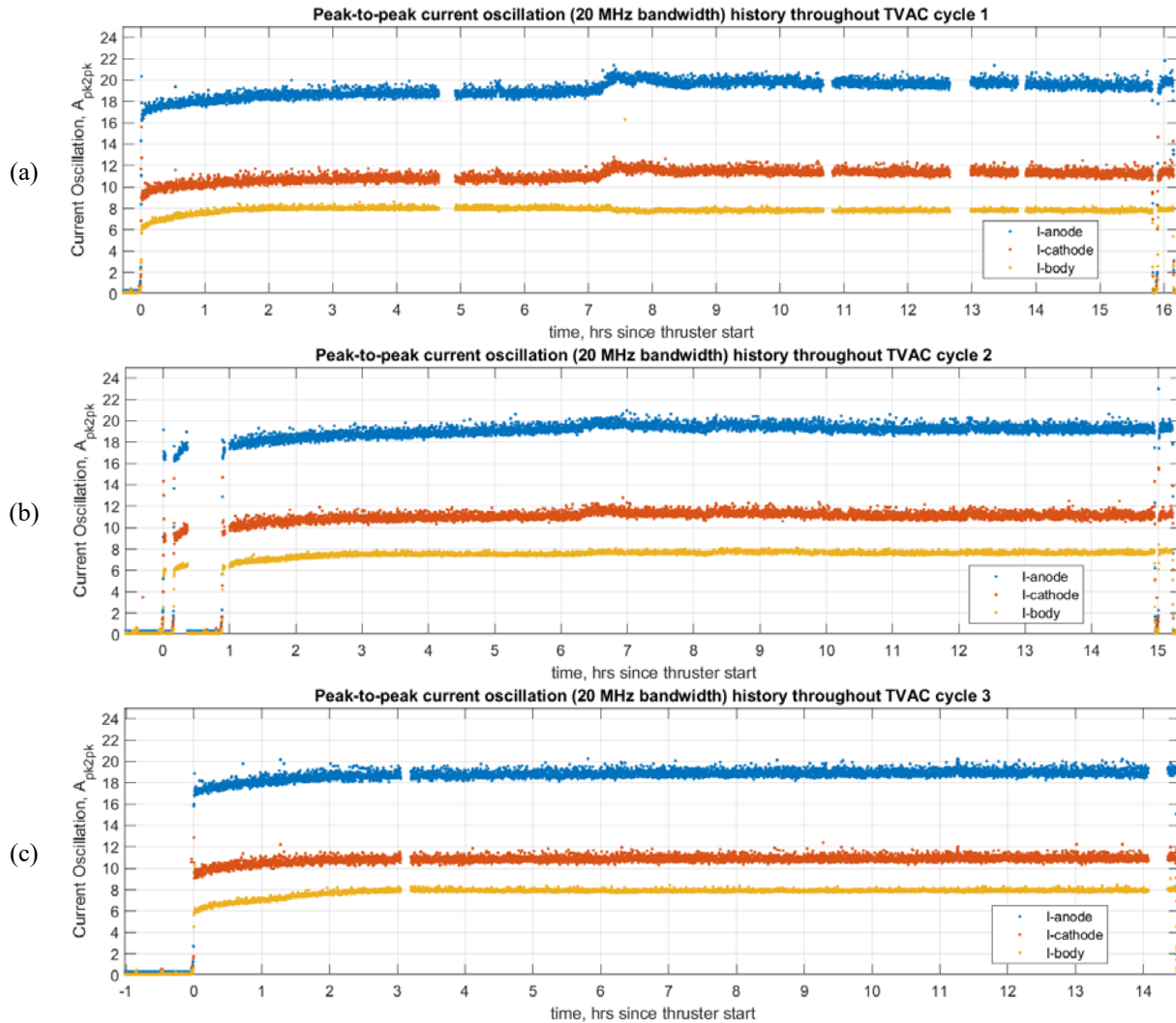
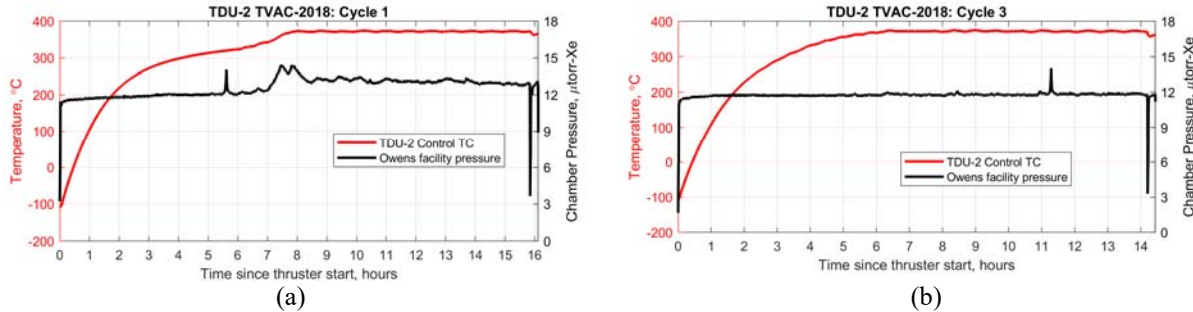


**Figure 12. Discharge current oscillation peak-to-peak magnitudes throughout TVAC (a) cycle 1, (b) cycle 2, and (c) cycle 3.**

The thruster high-speed dynamics were also recorded throughout all three TVAC cycles and the variations in the peak-to-peak currents (anode, cathode, and body) are shown in Figure 12. In all three cycles, the discharge current oscillation magnitude is slightly lower when the thruster is cold started at  $-121^\circ\text{C}$  ( $17.3 A_{\text{anode, pk2pk}}$ ) and gradually increases on average by 11.2% to  $19.2 A_{\text{anode, pk2pk}}$  at  $+373^\circ\text{C}$ . The peak-to-peak current data in Figure 12 represent the maximum minus the minimum current measured with 20 MHz bandwidth during a 0.5 second window. Occasionally, the scope logging software locked up and portions of data were missed (hence the gaps in the data). Also, all the cycles show the hot-restart at the end as a dropout and recovery—to the same amplitude—of the current oscillations. The two unexpected thruster shutdowns and restarts experienced during the 2<sup>nd</sup> cycle are also apparent in the data. While the 11.2% increase in current oscillations may appear large, the bulk of this change occurs within the first 3 hours of thruster operation (approximately  $-121^\circ\text{C}$  to  $+250^\circ\text{C}$ ) and remains at the same level indefinitely throughout the remainder of each cycle. The physical reason for the current amplitude variation is not readily clear and could be attributed to a variety of possible sources such as thruster component temperatures affecting neutral propellant speeds and ionization physics, or the overall facility pumprate and pressure variation with temperature. Studies with cooled

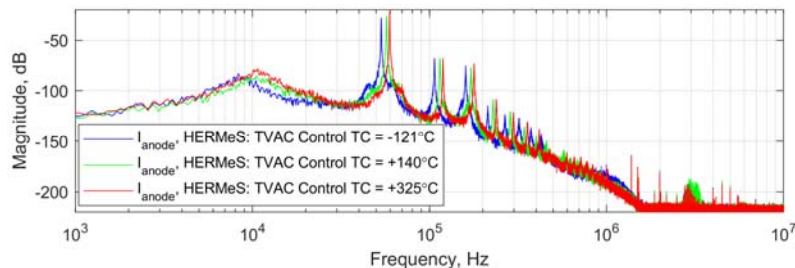
anodes (and thus slower neutral propellant)—while leading to improved performance [11]—have actually shown increased current oscillation amplitudes in Hall thrusters [12].

Figure 13 plots the cycle 1 and 2 variations in chamber pressure observed as the TDU-2 and TVAC shroud warmed from  $-121^{\circ}\text{C}$  to  $+373^{\circ}\text{C}$ . The 1<sup>st</sup> cycle shows an approximately 11.3% increase in chamber pressure that curiously tracks the current oscillation amplitude, while the 2<sup>nd</sup> (not shown) and 3<sup>rd</sup> cycles show 14.5% and 5.8% pressure increases respectively. In light of these data, it seems probable that the neutral background pressure is the key variable affecting the oscillation amplitude variations observed. By the 3<sup>rd</sup> TVAC cycle the facility pressure variations have lessened considerably as a likely consequence of a more fully outgassed TVAC shroud assembly. During the TVAC cycles these minor pressure changes were being actively tracked and corresponding RGA data also showed increased xenon and non-xenon partial pressures during heat lamp activation in cycles 1 and 2.



**Figure 13. Thruster temperature and facility pressure variations during TVAC (a) cycle 1, and (b) cycle 3 showing subsided facility pressure effects with temperature as the TVAC shroud appears of have completed outgassing.**

In addition to the high-speed oscillation amplitudes, full scope traces were captured throughout each of the TVAC cycles at an approximate rate of once per hour. The anode discharge current power spectral densities are included in Figure 14 for three different TDU-2 Control TC temperatures. These data show subtle shifts in the main peaks, but the qualitative dynamic character of the signals are largely invariant throughout the TVAC cycles.



**Figure 14. Power spectral density plots of the anode current throughout TVAC test 1.**

## J. Thermal Modeling compared to TVAC thermal measurements

One of the major objectives of the TDU2 environmental test was to take advantage of the long periods of steady state at elevated temperatures to validate a thermal model of the thruster. A thermal model of TDU-2 existed prior to the start of testing but was based on testing performed in a separate facility with a slightly different thruster model TDU-1 [7], so it was advantageous to the authors to use more accurate data to better understand the thermal characteristics of the thruster. The TDU-2 thermal model was created in NX 11 Space Systems Thermal based on a mechanical model of the thruster. Some components were simplified or ignored in order to facilitate the development of the thermal model. For example, fasteners are not explicitly modeled but thermal contact conductances across these interfaces are based on references from previous work, so their effect is captured. However, these types of simplifications were done sparingly and the vast majority of the components in the thruster are present in the thermal model.

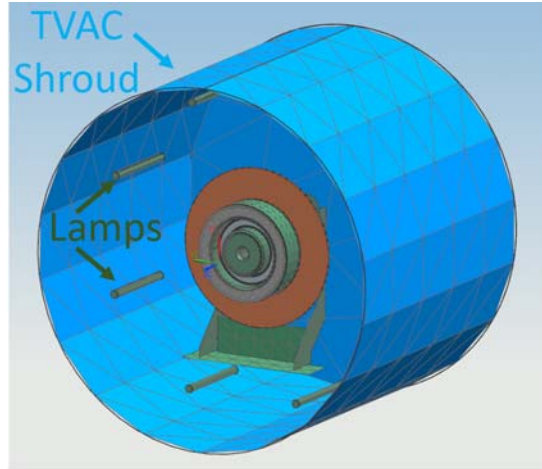


**Figure 15. Major component of the thermal model including the TDU-2 mounted inside the TVAC shroud with 8 heat lamps (used to increase the steady state hot-dwell temperature from 346°C to 373°C).**

The thermal model was validated in three main ways: (1) adjusting the assumed plasma loads from estimates provided by AEPS team member, Ioannis Mikellides, (2) modifying thermal contact conductances between components, and (3) modifying the optical properties of the components themselves. The primary method of validation was via the loads, but given that the thruster operates at relatively high temperatures for extended periods and understanding the realities of testing thrusters (accounting for carbon deposition, for example), the authors believe it is reasonable to expect variation in the thermal and optical properties of the thruster.

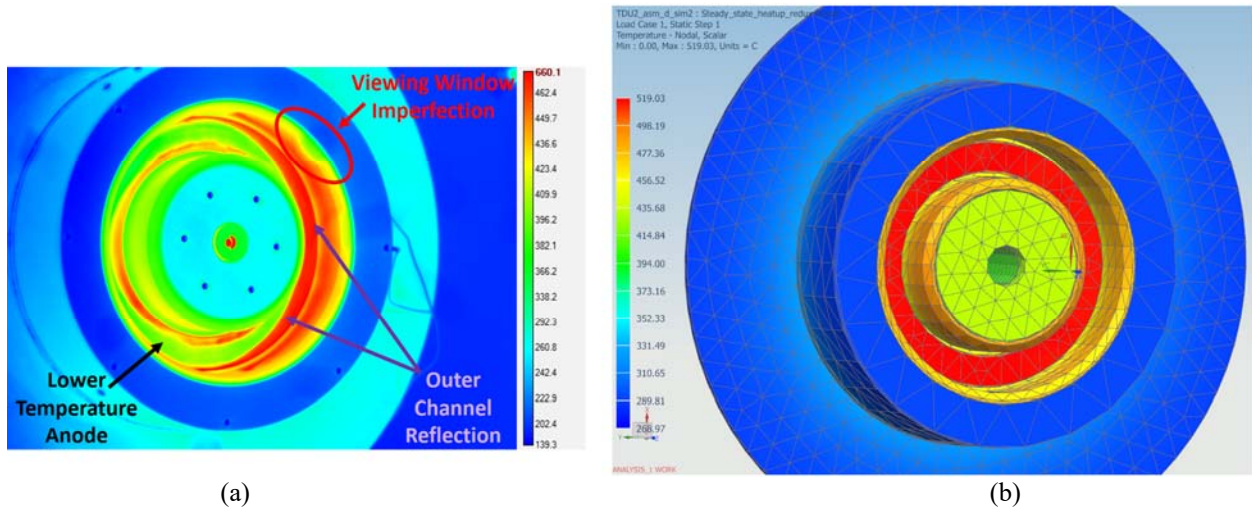


**Figure 16. (a) FLIR thermal camera image of thruster during 8-hour hot dwell of TVAC cycle 1. (b) Validated thermal model surface temperatures expected for the 8-hour hot dwell with the 600 V 12.5 kW thruster and  $\approx 5.4$  kW lamps running. NOTE: color scales do not match.**

The thermal model validation effort was concluded when the predicted thermal model values were within 10°C of the experimental thermocouple values (average difference is 5°C, and thermocouple accuracy for the measurements is  $\pm 3^\circ\text{C}$ ). IR thermography measurements were also taken of the thruster during operation and are compared to the thermal model in Figure 16, with relatively close agreement. The IR image has some differences from the thermal model, but the authors believe these differences are quantifiable. The IR image assumes every surface to be optically black (emissivity = 0.95) and observes reflections in the thruster and imperfections in the chamber viewing window that the thermal model does not account for. A more detailed description of the model validation efforts and error analysis will be presented in a later work.

**Table 3. List of experimentally measured temperatures (type-K thermocouples) compared to validated thermal model for 8-hour dwell condition when  $T_{control} = 373^{\circ}\text{C} \pm 3^{\circ}\text{C}$ .**

TC location	Experimental Data [°C]	Thermal Model Predictions [°C]	Error [°C]
TVAC shroud TC (upper)	223.4	227.4	4.1
TVAC shroud TC (lower)	230.5	227.0	-3.6
TDU-2 Control TC	372.1	378.6	6.5
TC 31 - INNER CORE	400.2	403.0	2.9
TC 30 - INNER SCREEN	406.5	403.0	-3.4
TC 29 - OUTER SCREEN	380.8	376.4	-4.4
TC 15 - BACK POLE NEAR ID (1)	377.7	378.6	1.0
TC 26 - OUTER FRONT POLE	295.4	289.8	-5.6
TC 43 - RADIATOR OD #2 (10)	241.7	288.8	-8.6
TC 04 - RADIATOR INSIDE SPOOL (8)	297.4	326.9	-4.7
TC 16 - FRONT POLE COVER 3:00 (14)	331.6	289.7	8.4
TC 09 - OUTER GUIDE 2:00 (7)	281.2	295.1	-7.1

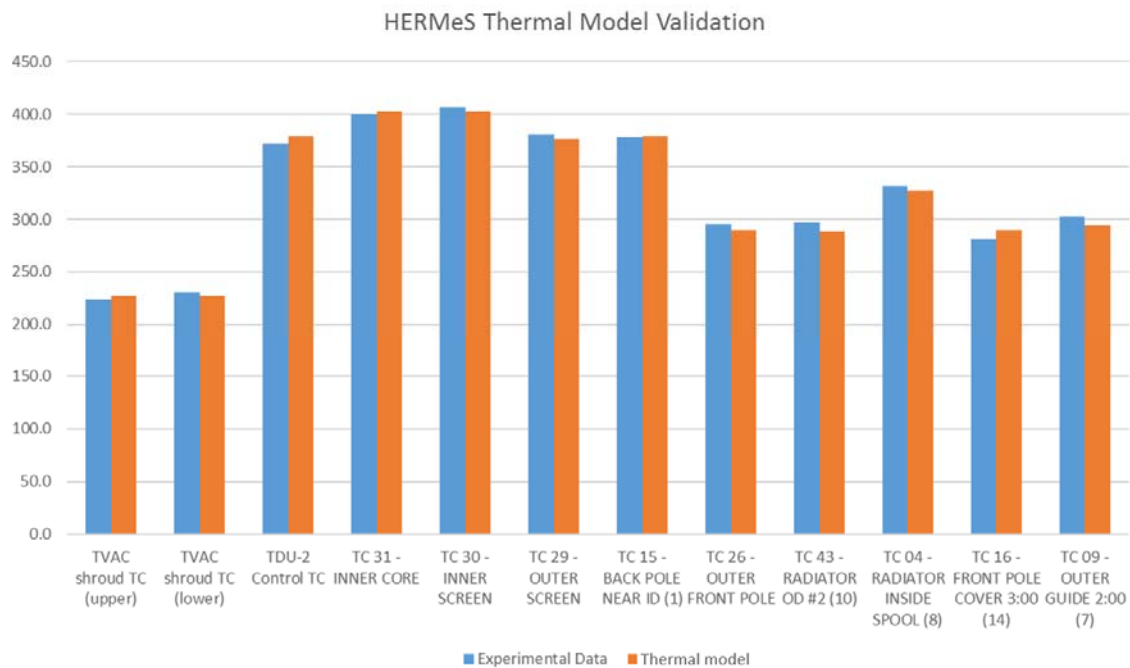


**Figure 17. Experimental versus modeled temperatures at different thruster locations during TVAC.**

### K. Thruster Performance and Characteristics

The initial JPL performance measurements with the TDU-2 thruster were conducted in 2016 when the thruster still had a boron nitride discharge channel ceramic [14]. Following the modification of the TDU-2 thruster with upgraded borosilicate ceramic, the performance was again measured during the pre-RV/TVAC characterization test at the start of the environmental test campaign laid out in Figure 4. Following the vibration and thermal environment testing, a post-RV/TVAC characterization test was conducted to track any performance changes that may have occurred. These performance data are listed in Table 4 where the average difference in pre- to post-RV/TVAC thrust was just 0.3%—

well within the measurement uncertainty—thereby qualifying the TDU-2 performance invariance and thruster compatibility with the conducted environmental testing.

**Table 4. TDU-2 Performance measurements pre-RV/TVAC and post-RV/TVAC along with boron nitride and borosilicate comparison.**

Voltage (Volts)	Current (Amps)	Power (kW)	Thrust: post-RV/TVAC borosilicate (mN)	Thrust: pre-RV/TVAC borosilicate (mN)	Thrust: pre-RV/TVAC boron nitride [14] (mN)	Uncertainty (mN)	Difference boron nitride to borosilicate (%)	Difference pre- to post-RV/TVAC (%)
300	20.83	6.2	394	395	398	±6 mN	-0.8%	-0.3%
400	20.83	8.3	479	480	483	±7 mN	-0.6%	-0.2%
500	20.83	10.4	550	548	552	±8 mN	-0.7%	0.3%
600	20.83	12.5	605	603	612	±9 mN	-1.5%	0.3%
700	17.83	12.5	561	562	570	±8 mN	-1.4%	-0.1%
500	25	12.5	643	645	651	±9 mN	-0.9%	-0.2%
300	10.3	3.1	184	183	186	±3 mN	-1.6%	0.5%
Ave.  diff.:							<b>1.1%</b>	<b>0.3%</b>

For the 20.83-A discharge current the thrust trend with voltage for all three conditions (boron nitride, borosilicate pre-RV/TVAC, and borosilicate post-RV/TVAC) is portrayed in Figure 18. While the pre- to post-RV/TVAC performance overlaps very closely, there does appear to be a slight decrease in performance with the borosilicate vs boron nitride channel walls. This slight decreased performance (~-1.5%) is largest at the highest discharge voltages of 600 and 700 V suggesting a possible plasma wall interaction effect that may involve the two different material secondary electron emission properties [15]. However, as a magnetically shielded thruster, the HEMReS TDU-2 should not have significant plasma wall contact [16] [17]. Regardless, the performance difference between the materials is still within the thrust measurement uncertainty.

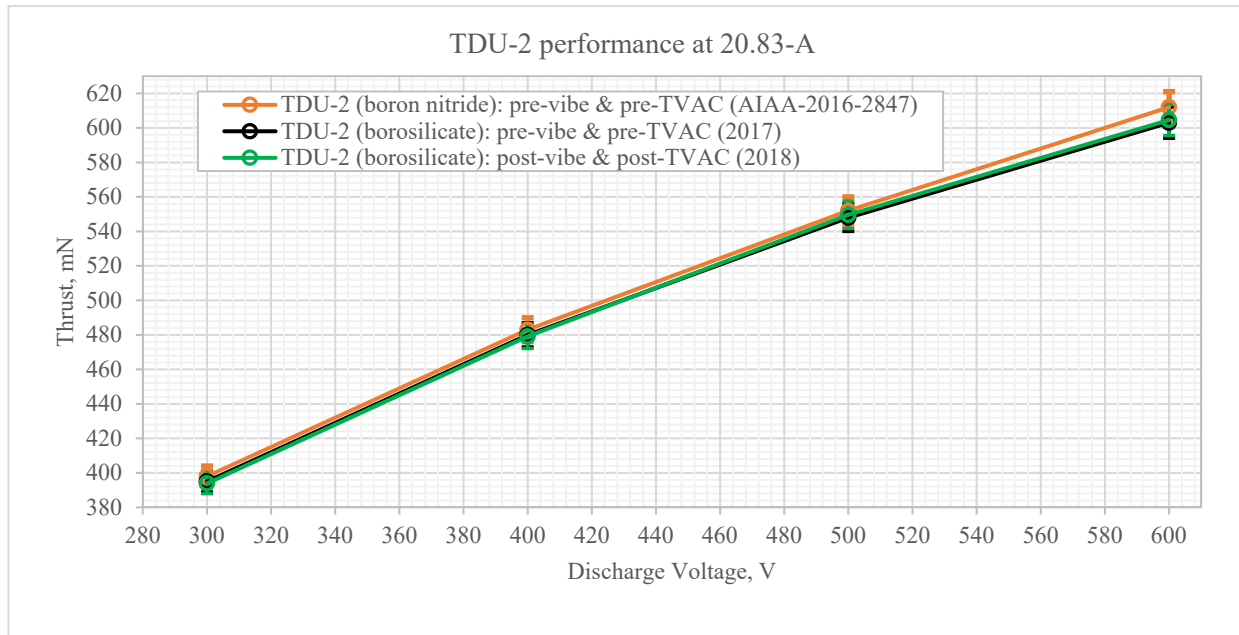


**Figure 18. TDU-2 20.83 A thrust profiles across discharge voltages from 300 V to 600 V for boron nitride pre-RV/TVAC (orange), borosilicate pre-RV/TVAC (black), and borosilicate post-RV/TVAC (green).**

Faraday probe scans were performed before and after the RV and TVAC testing with the results presented in Figure 19 for three different axial locations. The ion current profiles appear roughly invariant implying that the vibrational and thermal environmental testing of the TDU-2 hardware has no measurably significant effect on the plume divergence of the thruster.

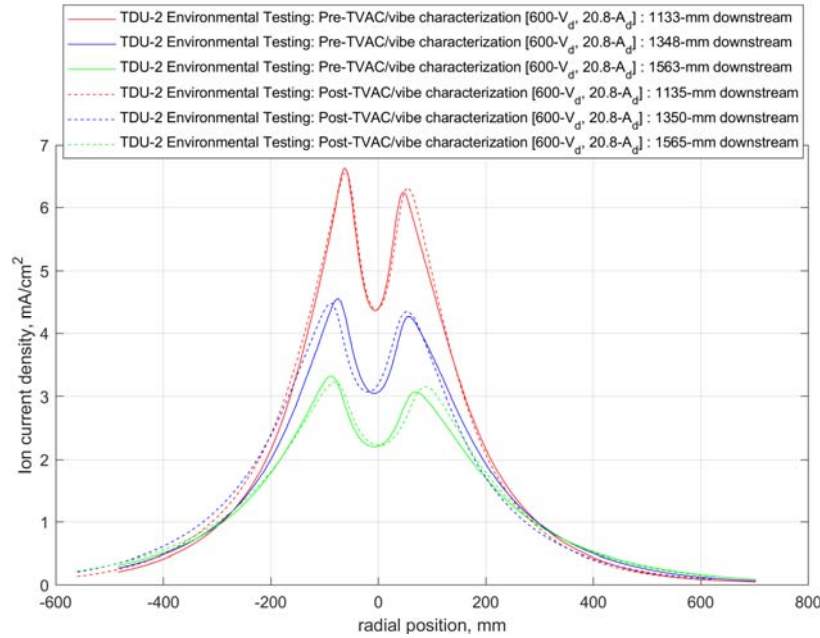


**Figure 19.** Set of TDU-2 Faraday probe scans at three different axial positions acquired before (—) and after (- - -) RV and TVAC testing.

Visually, the TDU-2 thruster underwent minor appearance changes throughout the environmental test campaign as depicted in Figure 20. The borosilicate ceramic darkened slightly after the TVAC testing which is characteristic for carbon backsputter from the ground testing of magnetically shielded Hall thrusters. The blue anodized aluminum thruster mounting bracket lost much of its color due to carbon backsputter as well as possible slight decomposition of this coating at the elevated TVAC testing temperatures. Various portions of the TVAC shroud gained a blue patina suggesting this later possibility. Detailed inspections of the TDU-2 before and after the RV/TVAC testing show no damage to the monolithic borosilicate channel and all ceramic to magnetic circuit gaps measured within tolerance.

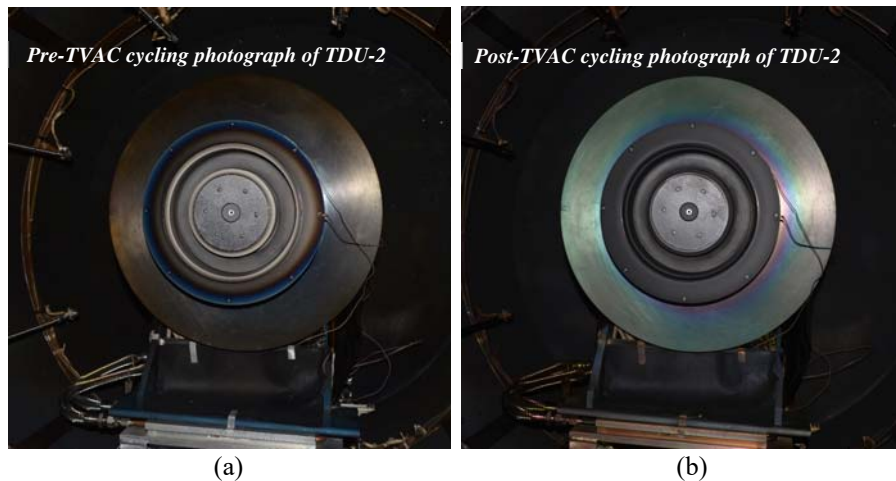


**Figure 20.** (a) Photograph of TDU-2 prior to start to TVAC testing compared to photograph of TDU-2 after the successful completion of 3 full TVAC cycles from  $-121^{\circ}\text{C}$  to  $+373^{\circ}\text{C}$ .

## IV. Conclusion

The HERMeS TDU-2 thruster has successfully completed random vibrational and thermal vacuum qualification testing. An initial round of vibrational testing revealed several design weaknesses (dust and deformation) that once addressed allowed the TDU-2 to survive the full load schedule of 10  $g_{rms}$  over 120 seconds in each axis with only minor structural signature changes and negligible particulate generation. The thermal vacuum testing also required two attempts after an inadequately designed GSE harness melted and failed. After a more robust harness was built and tested, three thermal vacuum cycles were fully executed and minimal thruster operational variances were observed ( $\pm 0.2^\circ$  thrust vector angle changes, +11% current oscillation amplitude increase, and slight oscillation spectral shifts) as the thruster operated at full power 600-V 12.5-kW from  $-121^\circ\text{C}$  to  $+373^\circ\text{C}$ . A thermal model of the TDU-2 and TVAC test setup was developed to support this effort and this model was accurately validated to match the experimental test results within  $5^\circ\text{C}$ . Comparisons of the performance and plume divergence also show invariance (within the measurement uncertainties) between pre-vibe/TVAC and post-vibe/TVAC thruster testing. This environmental testing campaign has paved the path for the EDU version of this thruster that shall be fully qualified in the near future using the lessons learned from this effort. Overall, the TDU-2 thruster—the largest and highest-power magnetically-shielded Hall thruster ever to undergo vibrational and thermal environmental qualification testing—has demonstrated that it appears likely to be capable of surviving the launch and deep space environments needed to support future NASA missions.

## Acknowledgments

The research detailed in this article was performed at the Jet Propulsion Laboratory, California Institute of Technology, under a contract with the National Aeronautics and Space Administration with funding from the AEPS program. The support of the joint NASA GRC and JPL development of HERMeS by NASA's Space Technology Mission Directorate through the Solar Electric Propulsion Technology Demonstration Mission project is gratefully acknowledged. The HERMeS team members that have developed the TDU and EDU thrusters includes staff from multiple organizations including Glenn Research Center, the Jet Propulsion Laboratory, Aerojet Rocketdyne, and others.

## References

- [1] Snyder, J. S., Anderson, J. R., Noord, J. L. V., and Soulas, G. C., "Environmental Testing of NASA's Evolutionary Xenon Thruster Prototype Model 1 Reworked Ion Engine," *Journal of Propulsion and Power*, vol. 25, pp. 94–104, 2009.
- [2] Reilly, S. W., Sekerak, M. J., and Hofer, R. R., "Transient Thermal Analysis of the 12.5 kW HERMeS Hall Thruster," AIAA 2016-5024, 52nd AIAA/SAE/ASEE Joint Propulsion Conference, Salt Lake City, UT, July 2016.
- [3] Gates, M., "Power Propulsion Element Status for Lunar Orbital Platform-Gateway," HEO Committee of the NASA Advisory Council, NASA Headquarters, March 27, 2018.
- [4] Garner, C., Polk, J., Brophy, J., and Goodfellow, K., "Methods for cryopumping xenon," AIAA 96-3206, 32nd Joint Propulsion Conference and Exhibit, Buena Vista, FL, July 1, 1996.
- [5] Dankanich, J. W., Walker, M., Swiatek, M. W., and Yim, J. T., "Recommended Practice for Pressure Measurement and Calculation of Effective Pumping Speed in Electric Propulsion Testing," *Journal of Propulsion and Power*, vol. 33, pp. 668–680, Aug. 2016.
- [6] Hofer, R. R., Jorns, B. A., Polk, J. E., Mikellides, I. G., and Snyder, J. S., "Wear test of a magnetically shielded Hall thruster at 3000 seconds specific impulse," IEPC-2013-033, Presented at the 33rd International Electric Propulsion Conference, The George Washington University, Washington, D. C., October 6, 2013.
- [7] Delgado, J. J., "Qualification of the SPT-140 for use on Western Spacecraft," AIAA 2014-3606, 50th AIAA/ASME/SAE/ASEE Joint Propulsion Conference, Cleveland, OH, July 28, 2014.
- [8] "Assembly and Subsystem Level Environmental Verification, Rev. 5," JPL Official Standard 60133 (D-35492), 2013.

- [9] Polk, J., Anderson, J., and Brophy, J., "Behavior of the thrust vector in the NSTAR ion thruster," AIAA-1998-3940, 34th AIAA/ASME/SAE/ASEE Joint Propulsion Conference and Exhibit, Cleveland, OH, July 13, 1998.
- [10] Snyder, J., Goebel, D., Hofer, R., Polk, J., Wallace, N., and Simpson, H., "Performance Evaluation of the T6 Ion Engine," AIAA-2010-7114, 46th AIAA/ASME/SAE/ASEE Joint Propulsion Conference & Exhibit, Nashville, TN, July 25, 2010.
- [11] Wilbur, P. J., and Brophy, J. R., "The effect of discharge chamber wall temperature on ion thruster performance," *AIAA Journal*, vol. 24, pp. 278–283, Feb. 1986.
- [12] Book, C. F., and R. Walker, M. L., "Effect of Anode Temperature on Hall Thruster Performance," *Journal of Propulsion and Power*, vol. 26, pp. 1036–1044, 2010.
- [13] Myers, J. L., Kamhawi, H., Yim, J., and Clayman, L., "Hall Thruster Thermal Modeling and Test Data Correlation," AIAA 2016-4535, 52nd AIAA/SAE/ASEE Joint Propulsion Conference, Salt Lake City, UT, July 22, 2016.
- [14] Conversano, R. W., Hofer, R. R., Sekerak, M. J., Kamhawi, H., and Peterson, P. Y., "Performance Comparison of the 12.5 kW HERMeS Hall Thruster Technology Demonstration Units," AIAA 2016-4827, 52nd AIAA/SAE/ASEE Joint Propulsion Conference, Salt Lake City, UT, July 25, 2016.
- [15] Raitsev, Y., Dourbal, P., and Spektor, R., "Secondary Electron Emission Properties of Boron Nitride Ceramic Materials at High Temperatures," IEPC-2015-342, 34th International Electric Propulsion Conference, Hyogo-Kobe, Japan, July 4, 2015.
- [16] Mikellides, I. G., Katz, I., Hofer, R. R., and Goebel, D. M., "Magnetic shielding of a laboratory Hall thruster. I. Theory and validation," *Journal of Applied Physics*, vol. 115, p. 043303, Jan. 2014.
- [17] Hofer, R. R., Goebel, D. M., Mikellides, I. G., and Katz, I., "Magnetic shielding of a laboratory Hall thruster. II. Experiments," *Journal of Applied Physics*, vol. 115, p. 043304, Jan. 2014.